Journal of Da-Yeh University, Vol. 10, No. 1, pp. 41-50 (2001)

Satellite Hydrazine Propulsion System Design Trades

AN-SHIK YANG
Department of Mechanical Engineering, Da-Yeh University
112, Shan-Jeau Rd., Da-Tsuen, Chang-Hwa, Taiwan

ABSTRACT

Numerical simulations have been conducted to investigate the effects of various key design parameters on the transport behavior of the propellant flow for a hydrazine-based satellite propulsion system. The flow-channel network numerical scheme was used to determine the blowdown curves for characterizing the propulsive performance of typical 500 kg-class small satellites at different tank sizes and thrust values. This study covers tank volumes from 91 l to 104 l and thrust forces from 1 N to 8.896 N. In order to explore the response of transient propagating waves, a theoretical model in conjunction with the method of characteristics (MOC) was solved numerically to obtain the pressure and propellant mass flowrate histories at various thrust levels and different total pipeline lengths. The predicted results indicate that larger amplitudes of pressure oscillations are observed for the situation of higher thrusts. For different total pipeline lengths, the Fourier spectrum analysis reveals that a longer pipeline shows a lower first-mode frequency with a higher spectral intensity as a trend.
Key Words **:** monopropellant hydrazine propulsion, fluid-hammer effect

衛星聯胺推進系統之設計

楊安石
大葉大學機械工程學系
彰化縣大村鄉山腳路 112 號

摘　要

本研究針對衛星聯胺推進系統進行推進劑流動特性之數值模擬，以探討當推進系統在配備不同推力等級之推進器，以及不同總管長條件下對系統流動特性的影響。在穩態流動分析部分，本文以流道網路法來研究系統之沖壓特性；在暫態流動分析部分，以特徵線法（MOC）來探討系統暫態壓力與流量隨閥件開關之變化情形。計算結果顯示，較大推力狀況將引致幅度較高之液鎚壓力昇高；而應用富立葉頻譜分析呈現總管長加長之推進劑流將降低第一模式頻率值，但同時也增益其頻譜強度。
關鍵詞：推進系統，液鎚效應

I. INTRODUCTION

Hydrazine propulsion system is widely used to provide the required impulse for satellite orbit transfer and attitude control due to its advantages of low cost, technical simplicity, high reliability, and relative stability under normal storage. [16] A hydrazine propulsion system consists of hydrazine thrusters to produce thrust, a propellant tank to store propellant, and various components and assemblies (such as latching isolation valves, pressure transducer, filter, fill/drain valves, and plumbing) associated with conditioning, controlling, and transferring propellant. It is furnished as a module that is readily integrated into a satellite for fitting a broad range of requirements with lightweight construction. [4, 6, 14]

A hydrazine propulsion system normally functions in a blowdown manner. A propellant/pressurant tank with a built-in propellant management device (PMD) is used to ensure a steady supply of gas-free propellant under all satellite orientations. The high-pressure pressurant gas (nitrogen or helium) provides a pressure force to drive the liquid propellant (hydrazine) flowing from the tank to the thrusters. As the liquid propellant is expelled from the tank, the pressurant pressure drops throughout the lifetime of propellant usage. A blowdown hydrazine propulsion system operates in either continuous or pulse mode. In the continuous mode operation, thrusters burn for an extended time period depending on different thruster characteristics. Since the propulsion performance parameters (such as thrust and specific impulse) are strongly affected by the system pressure, the determination of blowdown pressure profile for the whole lifetime period during propellant usage is one of major concerns in propulsion system design.

In the pulse-mode operation, thrusters are fired in a succession of on-off fashion to produce a series of impulse bits. Various approaches have been proposed for satellite attitude control with pulse-mode thruster firing. Pulse modulators, the most common approach, generate a pulse command sequence to the thruster valves by adjusting pulse width and/or pulse frequency, which can provide the benefits of better propellant economy, smoother control action, and closer to linear actuation. [1-3] The shut-off motion of the thruster valve can simultaneously introduce fluid-hammer (equivalent to water-hammer) pressure spikes in the pipe. For this kind of operation, the magnitude of fluid-hammer pressure spikes must be considered in a propulsion design to assure the system integrity. [7, 10] In probing the transport behavior of a transient pulsating laminar pipe flow, the conventional steady state Darcy friction formula may cause a significant error in simulating the strong damping of flow and pressure waves traveling through fluid lines. Zielke [18] developed a modified MOC including the effect of frequency-dependence friction term. The calculated results demonstrated accurate predictions of the response pressure fluctuations due to an instantaneous valve closure. Trikha [15] improved the Zielke's model to enhance its computational efficiency substantially. Schohl [11] further employed the least square fitting method for extending its applicable range with a better prediction accuracy.

In the past, most of research works related to monopropellant propulsion systems were focused on the propulsion characteristics of thrusters. Limited studies have been addressed on the steady state and transient flow phenomena of a hydrazine propulsion system. The pressurant and propellant flow in a hydrazine propulsion system can be numerically simulated to describe the flow and pressure balance in the propellant path through the system. This type of analysis can generally characterize the propellant mass flowrate and component/line pressure loss with respect to the tank pressure as well as the propellant flow transient properties, which are very crucial to the propulsion module design. The purpose of this paper is to perform the design analysis for hydrazine propulsion system, specifically studying the effects of various design variables, such as tank volume, thrust force level, flow resistance of components, total pipeline length, and duration setting of pulse trains, on the propulsion system performance.

II. THEORETICAL FORMULATION

In the present work, the design configuration of the ROCSAT-1 hydrazine propulsion system (with a schematic diagram and the pipeline data are shown in Fig. 1 and Table 1, respectively) is adopted as an illustration case. ROCSAT-1, launched on January 27, 1999, is a low-earth orbit scientific experimental satellite. This satellite encircles the Earth at an altitude of 600 km with an inclination angle of 35 degrees. The scientific experiments conducted on ROCSAT-1 include ocean color imaging, experiments on ionospheric plasma and electrodynamics, and experiments using Ka-band communication payloads. [8] The on-board hydrazine propulsion system is mainly used for orbit corrections at the final operational orbit and for attitude control during orbit insertion and contingency modes of operation.

1. Steady State Modeling

The present mathematical model considers ROCSAT-1 monopropellant feed system with various in-line components including a propellant tank, a filter, an orifice, a latching isolation valve, and four thrusters. The pressurant (namely

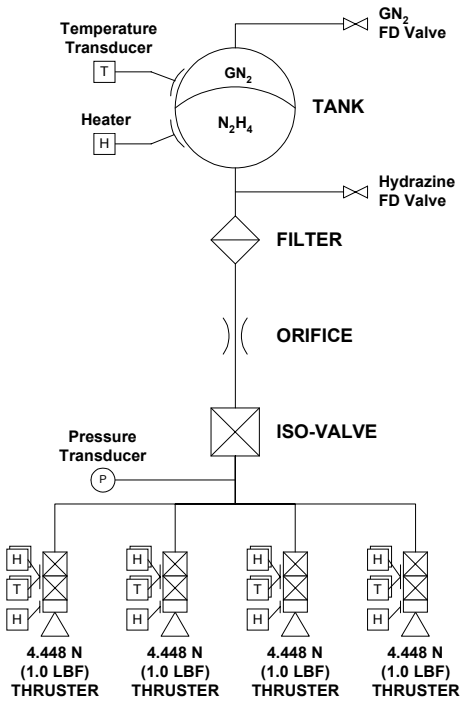

Fig. 1. Schematic of ROCSAT-1 propulsion subsytem

Table 1. Pipeline length and tube bend data for ROCSAT-1 RCS

No.	From	To	Length (mm)	Number of Bending Angles				
				22.5°	67.5°	90.0°	135.0°	157.5°
1	Tank	Filter	845	3	0	4	0	0
2	Filter	Orifice	203	0	0	1	0	1
3	Orifice	ISO-Valve	237	0	0	1	0	0
4	ISO-Valve	TJ #1	647	3	2	0	1	0
5	TJ #1	TJ #2	47	0	0	0	0	0
6	TJ #1	TJ #3	468	3	0	0	0	0
7	TJ #2	DTM #1	700	3	0	2	0	0
8	TJ #2	DTM #4	1122	6	0	3	0	0
9	TJ #3	DTM #2	700	3	0	2	0	0
10	TJ #3	DTM #3	1113	6	0	3	0	0

nitrogen) is used to pressurize the hydrazine propellant. To simulate the blowdown behavior of a single-phase liquid propellant feed system, the conservation equations of mass and momentum are formulated and solved numerically using the flow-channel network numerical method. The volume of pressurant is first estimated based on an initially guessed value of propellant mass flowrate. The pressurant pressure is then calculated by the ideal-gas equation. As the propellant flows through the pipelines and components, the pressure drop along pipeline and across each component at a certain mass flowrate can be computed employing the associated friction correlations. With the momentum equation, the thruster inlet pressure is readily obtained and can be in-turn applied to determine the propellant mass flowrate, thrust force, and specific impulse from the known characteristics of the thruster. Since the pressure drop is strongly coupled with the propellant mass flowrate, an iteration procedure is required to achieve a converged solution.

The governing equations used in the steady state modeling are given as below.

A. Tank region:

$$V = V_o + \int_0^t \frac{\dot{m}_{prop}}{\rho} dt \qquad (1)$$

$$T = T_o \qquad (2)$$

$$P = nRT / V \qquad (3)$$

Where V_o is the initial volume of the pressurant.

B. Pressure drop along the propellant lines:

$$P_t - P_u = \Delta P_p + \Delta P_f + \Delta P_{or} + \Delta P_{lv} \qquad (4)$$

C. Line Pressure Drop:

$$\Delta P_p = \frac{\rho v^2}{2}\left(\frac{fL}{D} + \sum k\right) \qquad (5)$$

Where $f = 64 / Re_D$. The term $\sum k$ stands for friction loss coefficients based on theoretical estimates for tees, miter bends, and elbows.

D. Filter pressure drop:

$$\Delta P_f = \frac{\rho v^2}{2} K_f \qquad (6)$$

E. Orifice pressure drop:

$$\Delta P_{or} = \frac{\rho v^2}{2} K_{or} \qquad (7)$$

F. Latching valve pressure drop:

$$\Delta P_{lv} = \frac{\rho v^2}{2} K_{lv} \qquad (8)$$

Where K_f, K_{or}, and K_{lv} are functions of propellant mass flowrate and can be obtained from component-level experimental correlation data. [9]

G. Thruster characteristics:

From the hot-firing test data, the thruster characteristics including the propellant mass flowrate, the thrust, and the specific impulse can be correlated with the inlet pressure of the thruster [9], namely:

$$\begin{cases} \dot{m}_{prop} = f[P_u] \\ F = g[P_u] \\ I_{sp} = h[P_u] \end{cases} \quad (9)$$

2. Transient Modeling

The time-dependent transport behavior modeling of the propellant in ROCSAT-1 hydrazine propulsion system is studied in this work. The following governing equations used in the present study are given as follows. More detailed formulation can be found in Ref. 13.

A. Continuity equation:

$$\frac{1}{\rho a^2}\frac{DP}{Dt} + \frac{\partial u}{\partial x} + \frac{u\sigma}{A} = 0 \quad (10)$$

where σ stands for the change rate of cross-sectional area along the x-direction, that is $\sigma(x) = \partial A/\partial x$. The acoustic speed can be determined by

$$a = \left[\frac{K/\rho}{1 + C(KD)/Ee}\right]^{1/2} \quad (11)$$

C is a function of Poisson's ratio whose form depends on the pipe restraint conditions.

B. Momentum equation:

$$\rho\frac{\partial u}{\partial t} + \rho u\frac{\partial u}{\partial x} = -\frac{\partial P}{\partial x} - \rho g\sin\alpha - \frac{\tau_w A_p \cos\theta}{Adx} \quad (12)$$

The fluid is considered to be slightly compressible with high bulk modules, and the relationship between the fluid density and the pressure is given by

$$\frac{dP}{d\rho} = \frac{K}{\rho} \quad \text{or} \quad P = P_0 + K\ln\frac{\rho}{\rho_0} \quad (13)$$

The equations of the conservation of mass and momentum establish a set of hyperbolic-type partial differential equations, and the method of characteristics (MOC) can be applied to analyze this fluid transient problem. When Eqs. (9) and (11) are transformed by the MOC, the velocity, pressure, density, and acoustic speed in terms of x and t can be solved by the following sets of ordinary differential equations:

$$C^+ : \begin{cases} \dfrac{dx}{dt} = u + a \\ \dfrac{1}{\rho a}\dfrac{dP}{dt} + \dfrac{du}{dt} + g\sin\alpha + \dfrac{A_p\tau_w\cos\theta}{A\rho dx} + \dfrac{ua}{A}\sigma(x) = 0 \end{cases} \quad (14)$$

and

$$C^- : \begin{cases} \dfrac{dx}{dt} = u - a \\ \dfrac{1}{\rho a}\dfrac{dP}{dt} - \dfrac{du}{dt} - g\sin\alpha - \dfrac{A_p\tau_w\cos\theta}{A\rho dx} + \dfrac{ua}{A}\sigma(x) = 0 \end{cases} \quad (15)$$

In modeling the frequency-dependent frictional losses of the unsteady laminar pipe flow, the wall shear stress (τ_w) can be related to the instantaneous mean velocity and the weighted past velocity change. In the present work, an eight-term approximate function is proposed in conjunction with the use of a nonlinear least square approach to increase the computation efficiency and avoid the massive storage of the entire flow history while computing the weighted past velocity change.

The initial condition of simulation is obtained by solving the following equations:

$$\begin{cases} \dfrac{1}{\rho a^2}\dfrac{dP}{dx} + \dfrac{1}{A}\sigma(x) + \dfrac{1}{u}\dfrac{du}{dx} = 0 \\ \dfrac{dP}{dx} + \rho u\dfrac{du}{dx} + \rho g\sin\alpha + \dfrac{A_p\tau_w\cos\theta}{Adx} = 0 \end{cases} \quad (16)$$

The pressure at the tank outlet is set to be a constant of 24.5 bar, and the thruster inlet velocity at $t = 0^+$ is 0 m/sec due to the sudden closure of the valve.

III. RESULTS AND DISCUSSION

An experimental propellant feed system was established to conduct the blowdown experiment for measuring a continuous pressure drop of the pressurant as the propellant was discharged continuously. The experimental data was obtained to validate the present steady state computer program. The comparison results have demonstrated excellent agreement between the calculated and measured pressure-time histories at the locations of the propellant tank and the thruster inlet. More detailed information can be found in Ref. 5. For the time-dependent flow study, the transient flow formulation jointly with the method of characteristics was verified by

comparing with Simpson's experimental data [12]. A long straight pipe was set up horizontally with the mounting of an upstream constant-pressure tank and a downstream fast-closing ball valve. The pressure waves were generated due to the closing of the downstream ball valve (with the valve closure time of 0.015 sec). The predictions were found to agree well with the pressure-wave measurements. [17]

Numerical simulations were conducted for the following baseline condition. The total internal volume of the propellant tank is 0.091 m^3 with a qualified propellant storage capacity of 72.6 kg. Nitrogen is used to pressurize the hydrazine propellant with the initial pressure of 24.5 bar. All lines from the tank outlet to the inlet of thruster valves are first filled with hydrazine. Since the propellant tank is externally covered by multi-layer insulation with heaters attached for the temperature control, the temperatures of pressurant and propellant are nearly same and can reasonably stay quite constant during the mission. In computation, the temperature of nitrogen and hydrazine is set to be T_0 with a nominal value of 15.6°C, which is an orbital average temperature for imitating in-orbit situations.

In this analysis, four thrusters are considered to be firing simultaneously in the steady state operation mode over the blowdown pressure range. The effects of tank expansion, hydrazine vapor pressure, and solubility are neglected. The friction coefficients K_f, K_{or}, and K_{lv} (shown in Eqs. (6), (7), and (8)) are computed by linear approximation of the working points given in the component equipment specifications. These working points of the pressure drop/mass flowrate relationship for each propulsion component are listed as follows: 1) filter: 7560.0 Pa @ 7.576 g/sec; 2) orifice: 51900.0 Pa @ 7.576 g/sec; and 3) latching valve: 16400.0 Pa @ 7.576 g/sec. From the hot-firing acceptance test data at the vacuum condition for thrusters used in ROCSAT-1 program, the propellant mass flowrate passing through a 4.448-N (1-lbf) thruster is correlated to the thruster inlet pressure as the subsequent expression: $\dot{m}_{prop} = (2.222 \times 10^{-5}) \times P^{0.774}$, where the unit of $\dot{m}_{prop}$ and P is g/sec and Pa respectively.

To design a satellite hydrazine propulsion system, the trade-offs of various design features must be conducted based on mission requirements. The system will be then sized iteratively until the best configuration is attained. During the sizing process, the qualified capability ranges of key design parameters are examined in detail to properly configure tanks, thrusters, and flow components to be implemented in the propulsion system. The tank sizing process is first performed for the ROCSAT-1 hydrazine propulsion system. In this work, three potential tanks were considered with the tank volume of 91 l, 96 l, and 104 l, respectively. Main characteristics of those tanks are given in Table 2. Figure 2 shows the tank pressure profiles with respect to the remaining propellant mass for three different tanks. In calculations, three blowdown curves are based on the same initial tank pressure of 24.5 bar with the identical propellant loading on-board of 72.6 kg for all proposed tanks. Corresponding to the remaining hydrazine mass from 72.6 kg to null, the three predicted blowdown pressure profiles range from 24.5 bar at beginning-of-life (BOL) to 4.96 bar, 5.98 bar, and 7.40 bar at end-of-life (EOL) for the internal tank volume of 91 l, 96 l, and 104 l. For all three cases, the tank pressure in the early phase of the event reduces at a relatively faster rate than that at the later phase of the event. This is due to the fact that the pressurant occupies a lesser percentage of the internal volume of the tank in the beginning, while a greater pressure decrease can be introduced subsequently by the free volume produced through the propellant consumption in the tank. Compared with the pressure profile for a larger tank, the pressure for a smaller tank tends to drop relatively faster in the primitive development stage of the blowdown phenomenon. Therefore, for any fixed value of remaining hydrazine mass (shown in Fig. 2), it is clearly observed that the pressure for a bigger tank (e.g. the 104-l tank) is constantly greater than that for a smaller tank (the 91-l tank).

Table 2. Main characteristics of potential tanks considered in tank sizing process

	Tank 1	Tank 2	Tank 3
Supplier	PSI	DOWTY	DASA
Type	Diaphragm	Diaphragm	Surface tension
Shape	Spherical	Spherical	Spherical
Mass (kg)	6.7	8.2	6.4
Volume (liter)	91	96	104
Qualified Propellant Capacity (kg)	72.6	74.5	81.0

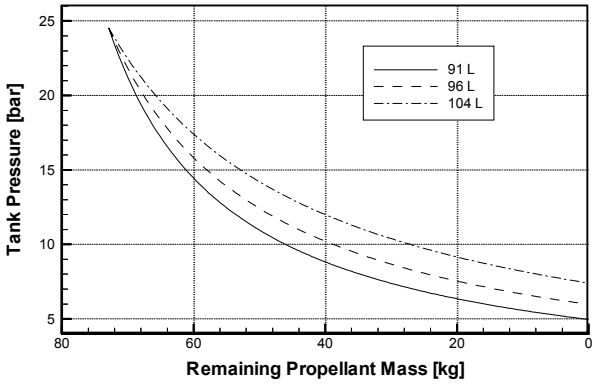

Fig. 2. Blowdown pressure profiles for three different tanks

Successively, the mass flowrate effect on the propulsive performance was conducted. Three different values of mass flowrate (corresponding to 1-N, 4.448-N (1-lbf), and 8.896-N (2-lbf) hydrazine thrusters) were examined in this study. These kinds of thrusters have been commonly utilized in the propulsion system of 500 kg-class low-earth-orbit (LEO) satellites. Figure 3 presents blowdown histories of the tank pressure and the remaining propellant mass along the mission duration at various thrust force levels. The remaining mass and tank pressure profiles stay relatively constant in the initial stage for all three cases. Since a larger propellant mass flowrate is required to sustain a continuous firing operation of thrusters with a higher thrust value, the hydrazine remaining mass and tank pressure curves for the 8.896-N case reduce substantially faster in comparison with those of the 1-N case. This observation suggests that the operation lifetime of using 8.896-N thrusters can be much shorter than that of using 1-N thrusters. The predicted time span values for the thrust force of 1 N, 4.448 N, and 8.896 N are 1580 min, 362 min, and 190 min throughout the lifetime of propellant usage. As displayed in Fig. 4, the total line pressure loss and thrust were also computed over the entire blowdown pressure range for three

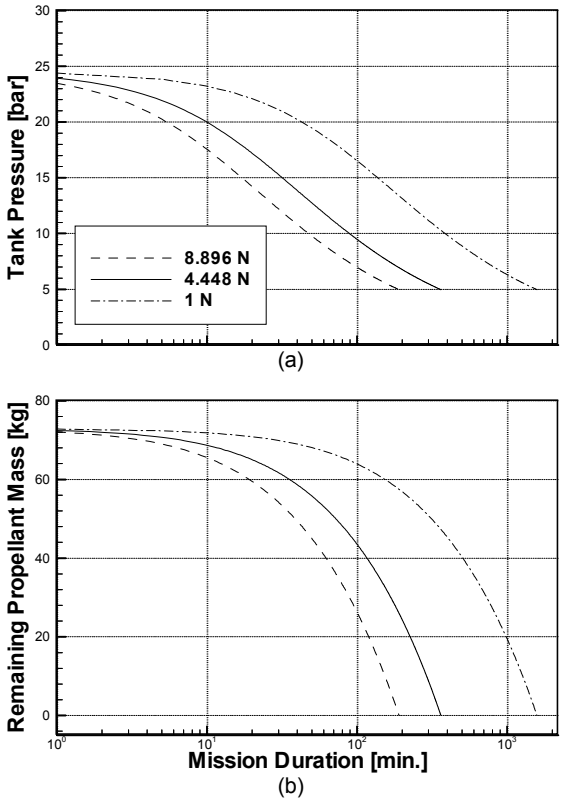

Fig. 3. Blowdown histories of (a) tank pressure and (b) remaining propellant mass along the mission duration at various thrust force levels

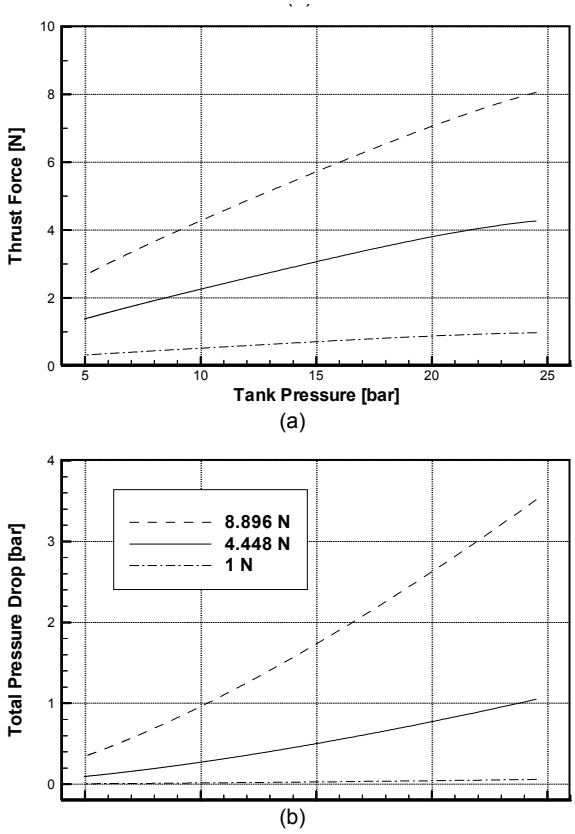

Fig. 4. (a) Thrust force and (b) total pressure loss over entire blowdown range for 1 N, 4.448 N and 8.896 N thrusters

examples. The total line pressure loss/thrust force at the maximum effective operating pressure (MEOP) of 24.5 bar are 3.51 bar/8.05 N, 1.05 bar/4.27 N, and 0.06 bar/0.98 N for the thrust level of 8.896 N, 4.448 N, and 1 N, respectively. Except the total pressure loss curve for the 8.896-N thruster, almost all profiles are about linearly proportional to the tank pressure. Due to its high propellant mass flowrate through the hydrazine supply line, the total line pressure loss for the case of 8.896-N thruster is 14.3% of MEOP at BOL. This considerable pressure loss leads to a substantial decrease of the upstream pressure at the thrust inlet, and in turn deteriorates the thrust output. For this calculation, the estimated thrust value at BOL is about 8.05 N, which is only 90% of the design thrust for a 8.896-N thruster. In practice, the requirement of maximum acceleration for satellite orbit maneuver can establish criteria of thruster sizing for a specific mission envelope. The qualified capability of operating lifetime should be also considered in thruster selections.

The influence of various design features on the time-dependent transport behavior of the satellite hydrazine propulsion system is also studied using an MOC-Based computer code. In simulations, all pipelines from the

propellant tank to thruster valves were initially primed with hydrazine at 24.5 bar. Three cases of valve operations are investigated in this study. Those are: (1) instantaneous closing of the latching isolation valve, (2) instantaneous closing of four thruster valves, and (3) pulse train with a series of iterative open-close operations for thruster valves. For evaluating the fluid-hammer effect under the worst situations, all thruster valves are considered to be opened and closed simultaneously.

Prior to the closure of the latching valve, the latching valve and thruster valves are at the 'open' position with a stable propellant flow through all pipelines. The latching isolation valve is then suddenly closed at $t = 0^+$ sec. Figure 5(a) shows the transient pressure responses at the inlet of the latching isolation valve for various thrust-force levels. Caused by the abrupt closure of the latching isolation valve, the pressure immediately builds up to its peak and evolves fluctuant waves due to the outcome of fluid hammer. The pressure responses act similar damping behavior for the other three thrust values with a nearly same decay time constant (defined as the time period of the amplitude ratio reducing from 1 to *1/e*) of 13.6 sec^{-1}. It exhibits that all pressure waves are damped out rapidly resulting from the surge-tank and friction effects. And these profiles converge toward their initial pressure of 24.5 bar within approximately 0.34 second. The maximum values of the predicted pressure rise for 1-N, 4.448-N, and 8.896-N thrusters are 0.94 bar, 4.18 bar, and 8.34 bar, respectively. Larger amplitudes of pressure oscillations are observed for the situation of higher thrusts. The pressure rise tends to be linearly proportional to the thrust level. It can be attributed that a higher thrust force would entail a larger propellant mass flowrate through the pipeline, and in turn lead to a greater pressure rise due to its stronger flow inertia.

Since it is only a minor difference for pipeline lengths from the common junction (in the downstream of the latching isolation valve) to four thrusters, the inlet pressure responses are almost identical for four thrusters in the propulsion module. Figure 5(b) illustrates the pressure histories at one of thruster valve inlets for three cases. The thruster valves were closed instantaneously and simultaneously at $t = 0^+$ sec. Similar to the results obtained in those cases of closing the latching isolation valve, the pressure profiles jump up to their first spike and oscillates with a larger value of the period for decay travelling sine waves. The pressure responses are then damped out quickly and approaching toward 24.5 bar. Because of a relatively longer pipeline length for these calculations, the magnitudes of the pressure fluctuations are somewhat lower compared with those cases of closing the latching isolation valve.

Characteristics of the transient pressure waves at the thruster valve inlet are further probed in this study. By transforming the pressure fluctuations from the time domain (as shown in Fig. 5(b)) to the frequency domain, various modes of pressure waves can be determined using the Fourier spectral analysis. In the structure analysis of the propulsion system,

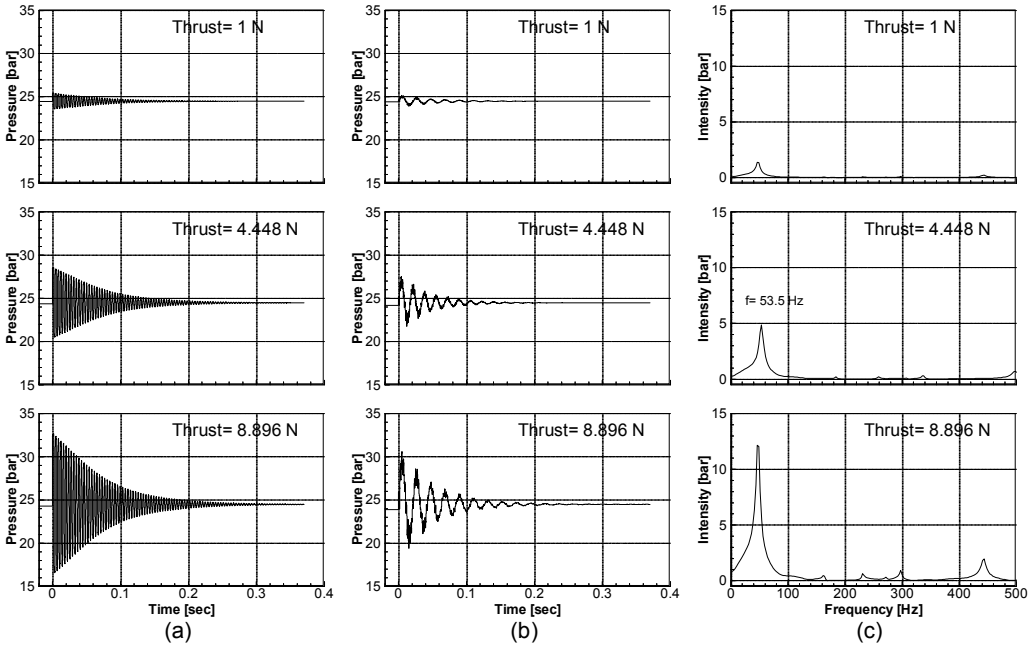

Fig. 5. Transient pressure at (a) latching isolation valve inlet and (b) thruster valve inlet for different thrust force levels, and (c) fourier spectral analysis of pressure valve at thruster valve inlet

the resonant frequencies of the thruster assembly and fuel lines are typically required to exceed 130 and 75 Hz for assuring the structure integrity. Figure 5(c) displays the results of the Fourier spectral analysis for the pressure fluctuations at the thruster valve inlet. For three cases, this plot clearly indicates a number of wave modes with the highest peak of intensity at the frequency of 53.5 Hz. This corresponding peak spectral intensity is found to increase with the thrust force level. In addition, the first-mode frequency of 53.5 Hz is substantially lower than the design resonant frequencies of thruster assembly and fuel lines stated in the hydrazine propulsion system design specifications. It can be then ensured that the induced excitation from the fluid-hammer pressure oscillations will not resonantly couple with the above-mentioned propulsion structure elements.

In this work, the effect of geometrical dimension on the time-dependent flow behavior was also studied. Three different pipeline lengths ($0.5L_o$, L_o, and $1.5L_o$) were considered in simulations where L_o denotes the total pipeline length of the ROCSAT-1 propulsion system. For different total pipeline lengths, Figure 6 presents the transient pressure histories at the latching isolation valve inlet and thruster valve inlet as well as the Fourier spectral plots of pressure waves at the thruster valve inlet. For all cases, the maximum pressure raises attained at the latching isolation valve inlet and thruster valve inlet are nearly same with the magnitude of 4.1 bar and 3.3 bar, indicating that the pressure raise is not sensitive to the change of pipeline length as the thrust force is determined. Since the frequency of the pressure response is equal to the acoustic speed divided by the travelling distance of the wave, a higher frequency of the pressure waves occurs for a shorter pipeline length. It can be then expected that, within a fixed time interval, the iterative number for the pressure wave propagating back and forth in a shorter pipeline is greater than that of a longer pipeline. This flow behavior can result in the stronger friction and surge-tank effects and successively lead to a more rapid decay rate of the damped pressure oscillation in a shorter pipeline. Therefore, the decay time constants of the damped pressure fluctuation at the latching isolation valve inlet are 23.1 sec^{-1} for $0.5L_o$, 13.8 sec^{-1} for L_o, and 10.4 sec^{-1} for $1.5L_o$, respectively. The pressure response in the time domain at the thruster valve inlet was further converted into the spectral intensity in the frequency domain through the Fourier spectrum analysis. As the total pipeline length increases, larger flow inertia mass is involved in a fluid vibratory system, which tends to lower the first-mode frequency and substantially augment its spectral intensity for a longer pipeline. It is also observed that the intensities at higher-mode frequencies for all cases are insignificant.

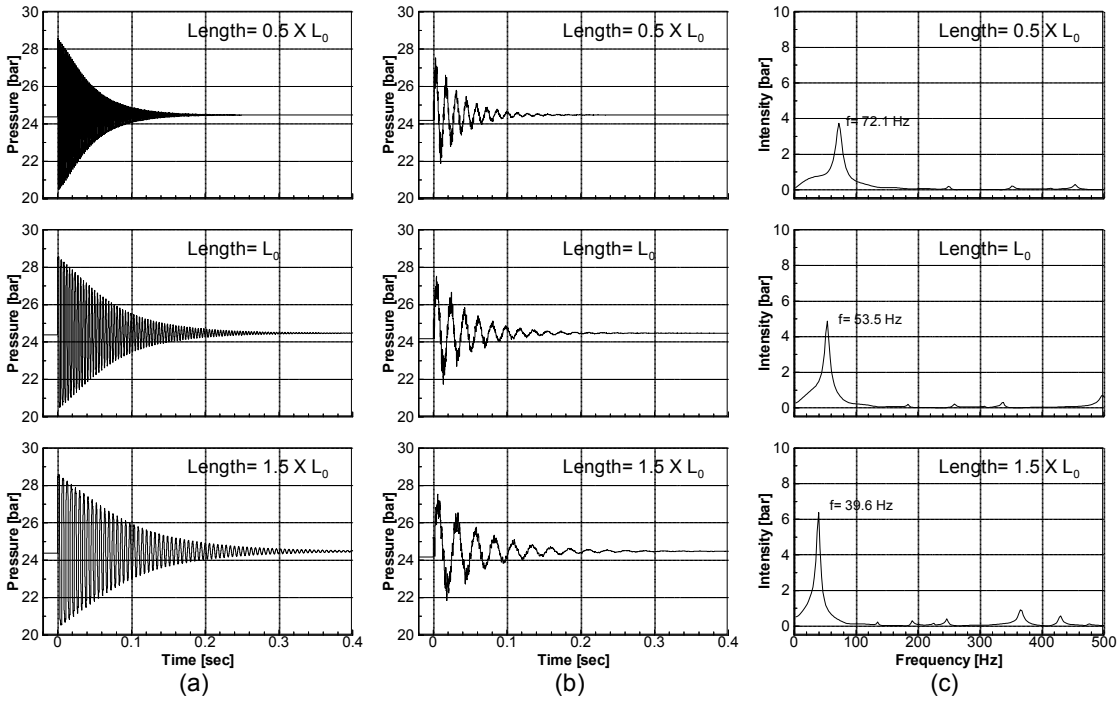

Fig. 6. Transient pressure at (a) latching isolation valve inlet and (b) thruster valve inlet for different pipe line lengths, and (c) fourier spectral analysis of pressure waves at thruster valve inlet

IV. CONCLUSIONS

The influence of various design features on the configuration of satellite hydrazine propulsion system has been studied using the numerical analysis. The flow-channel network computational scheme was employed for determining the blowdown characteristics at the tank volume and the thrust force ranging from 91 l to 104 l and 1 N to 8.896 N, respectively. The transient formulation was based on the conservation equations of mass and momentum to simulate the time-dependent transport behavior of the propellant flow. The governing equations were solved numerically using the method of characteristics (MOC) to obtain the traveling waves of pressure and mass flowrate.

In this study, the conditions were systematically varied in terms of thrust value, and total pipeline length. The fluid-hammer phenomenon is initiated immediately after the instantaneous valve closing. The pressure rise tends to be linearly proportional to the thrust values. The pressure waves are then diminished in a short period resulting from the friction and surge-tank effects. Simulations for different pipeline lengths were also conducted. Results indicate that larger flow inertia mass in the longer pipeline has a tendency to lower the first-mode frequency and augment its spectral intensity.

REFERENCES

1. Agrawal, B. N., R. S. Mcclelland and G. Song (1997) Attitude control of flexible spacecraft using pulse-width pulse-frequency modulated thrusters. *Space Technology*, 17(1), 15-34.
2. Bellerby, J. M. (1967) Hydrazine as a propellant for space systems. *Chemical System Group, Cranfield Institute of Technology*, Royal Military College of Science, Shrivenham, Swindon, Wilts.
3. Blazer, D. L., Y. C. Brill, W. R. Scott and P. Y. Sing (1976) The monopropellant hydrazine reaction control system for the RCA SATCOM satellite. AIAA/SEA 12th Propulsion Conference, AIAA Paper 76-631, 1976.
4. Hasan, D., S. Adler, A. Oren and N. Miller (1995) Propulsion systems for small satellites. *Space Technology*, 15(6), 375-381.
5. Hsieh, W. H., C. Y. Lin and A. S. Yang (1997) Blowdown and waterhammer behavior of monopropellant feed systems for satellite attitude and reaction control. 33rd AIAA/ASME/SEA/ASEE Joint Propulsion Conference, AIAA Paper 97-3224, Seattle, WA.
6. Huzel, D. K. and D. H. Huang (1992) Modern engineering for design of liquid propellant rocket engines. 174, Progress in Astronautics and Aeronautics, AIAA.
7. Molinsky, J. (1997) Water hammer test of the seastar hydrazine propulsion system. 33rd AIAA/ASME/SEA/ASEE Joint Propulsion Conference, AIAA Paper 97-3226, Seattle, WA.
8. Request for Proposal for the ROCSAT-1 Spacecraft, Document No. NSPO-RFP83-001, National Space Program Office, Hsinchu, Taiwan, December 8, 1993.
9. ROCSAT-1 Reaction Control Subsystem Design Report, Report No. DRL#31, TRW, Los Angeles, C.A., USA, 1995.
10. Sansevero, V. J. Jr. and H. Garfinkel (1976) Flight performance of the hydrazine reaction control subsystem for the communication technology satellite. AIAA/SEA 12th Propulsion Conference, AIAA Paper 76-630.
11. Schohl, G. A. (1993) Improved approximate method for simulating frequency-dependent friction in transient laminar flow. *Journal of Fluids Engineering*, 115(3), 420-424.
12. Simpson, A. R. (1986) *Large Water Hammer Pressure Due to Column Separation in Sloping Pipes*, Ph. D. Dissertation, University of Michigan, Ann Arbor, Michigan.
13. Steeter, V. L. and E. B. Wylie (1993) *Fluid Transients in System*, Prentice-Hill Book Co., New Jersey.
14. Sutton, G. P. (1992) *Rocket Propulsion Elements*, 6th Ed., John Wiley & Sons, Inc., New York.
15. Trikha, A. K. (1975) An efficient method for simulating frequency-dependent friction in transient liquid flow. *Journal of Fluids Engineering*, 97(1), 97-105.
16. Wertz, J. R. and W. J. Larson (1991) *Space Mission Analysis and Design*, 3rd Printing, Kluwer Academic Publishers, Dordrecht/Boston/London.
17. Yang, A. S. and T. C. Kuo (1997) Fluid analysis for determining flow coefficient of needle valve installed in RCS pressurization system. National Space Program Office, Report No. ROCSAT-1.SC86.206.
18. Zielke, W. (1968) Frequency-dependent friction in transient pipe flow. *Journal Basic Engineering*, Transactions ASME, Series D, 90(1), 109-115.

收件：90.03.09　修正：90.05.04　接受：90.05.15

NOMENCLATURE

A = pipe cross-sectional area
A_p = wetted peripheral area
a = acoustic speed
C = pipe anchored function
D = pipe diameter
E = Young's modules
e = pipe thickness
F = thrust
f = friction factor
g = acceleration of gravity
I_{sp} = specific impulse
K = bulk modules of fluid
k = loss coefficient
K_f = loss coefficient of filter
K_{or} = loss coefficient of orifice
K_{lv} = loss coefficient of latching valve
L = pipe length
$\dot{m}_{prop}$ = propellant mass flowrate
P = pressure
P_0 = reference pressure
P_t = tank pressure
P_u = thruster inlet pressure
ΔP_f = pressure drop across filter
ΔP_{lv} = pressure drop across latch valve
ΔP_{or} = pressure drop across orifice
ΔP_p = pressure drop across lines
R = gas constant
T = temperature
u = local mean velocity
V = pressurant volume
v = velocity
α = tilt angle of the pipe
θ = gradient of the pipe wall
ρ = density
ρ_0 = reference density
σ = area change rate
τ_w = wall shear stress